H3K4me1 marks DNA regions hypomethylated during aging in human stem and differentiated cells

H3K4me1 marks DNA regions hypomethylated during aging in human stem and differentiated cells

Agustín F Fernández, Gustavo F Bayón, Rocío G Urdinguio, et al.

Genome Res. published online September 30, 2014
Access the most recent version at doi:10.1101/gr.169011.113

H3K4me1 marks DNA regions hypomethylated during aging in human stem and differentiated cells

Agustín F. Fernández[1†*], Gustavo F. Bayón[1†], Rocío G. Urdinguio[1], Estela G. Toraño[1], María G. García[1]; Antonella Carella[1]; Sandra Petrus-Reurer[1], Cecilia Ferrero[1], Pablo Martinez-Camblor[2], Isabel Cubillo[3], Javier García-Castro[3], Jesús Delgado-Calle[4], Flor M. Pérez-Campo[4], José A. Riancho[4], Clara Bueno[5], Pablo Menéndez[5,6], Anouk Mentink[7], Katia Mareschi[8,9], Fabian Claire[10], Corrado Fagnani[11], Emanuela Medda[11], Virgilia Toccaceli[11], Sonia Brescianini[11], Sebastián Moran[12], Manel Esteller[6, 12, 13], Alexandra Stolzing[10,14], Jan de Boer[7,15], Lorenza Nisticò[11], Maria A. Stazi[11] and Mario F. Fraga[1,16*].

[1]Cancer Epigenetics Laboratory, Institute of Oncology of Asturias (IUOPA), HUCA, Universidad de Oviedo, Oviedo, Spain.
[2]Oficina de Investigación Biosanitaria (OIB-FICYT) de Asturias, Oviedo, Spain and Universidad Autónoma de Chile, Chile.
[3]Unidad de Biotecnología Celular. Área de Genética Humana. Instituto de Salud Carlos III.
[4]Department of Internal Medicine, Hospital U.M. Valdecilla, University of Cantabria, IDIVAL. Santander.
[5]Josep Carreras Leukemia Research Institute. School of Medicine. University of Barcelona. 08036. Barcelona. Spain
[6]Institut Català de Recerca i Estudis Avançats (ICREA). Barcelona. Spain.
[7]MIRA Institute of Biomedical Technology and Technical Medicine, University of Twente, Enschede, The Netherlands
[8]Pediatric Onco-Hematology, Stem Cell Transplantation and Cellular Therapy Division, City of Science and Health of Turin, Regina Margherita Children's Hospital; Turin, Italy
[9] Department of Public Health and Pediatrics, University of Turin, Italy
[10]Translational Centre for Regenerative Medicine, University Leipzig, Leipzig, Germany
[11]Genetic Epidemiology Unit; National Centre of Epidemiology, Surveillance and Health Promotion; Istituto Superiore di Sanità; Viale Regina Elena 299, 00161, Rome, Italy
[12]Cancer Epigenetics and Biology Program (PEBC), Bellvitge Biomedical Research Institute (IDIBELL), Barcelona, Catalonia, Spain.
[13]Department of Physiological Sciences II, School of Medicine, University of Barcelona, 08036 Barcelona, Catalonia, Spain.
[14]Loughborough University, Wolfson School of Mechanical and Manufacturing Engineering, Loughborough, UK
[15]cBITE laboratory, Merln Institute of Technology-inspired Regenerative Medicine, Maastricht University, Maastricht, The Netherlands
[16]Department of Immunology and Oncology, National Center for Biotechnology, CNB-CSIC, Cantoblanco, 28049 Madrid, Spain.

[†]Same contribution.

*Correspondence to:
Mario F. Fraga: mffraga@cnb.csic.es
Agustín F. Fernández: affernandez@hca.es

Short title: Epigenetic signatures of aging

Abstract

In differentiated cells, aging is associated with hypermethylation of DNA regions enriched in repressive histone posttranslational modifications. However, the chromatin marks associated with changes in DNA methylation in adult stem cells during lifetime are still largely unknown. Here, DNA methylation profiling of mesenchymal stem cells obtained from individuals aged 2 to 92 identified 18735 hypermethylated and 45407 hypomethylated CpG sites associated with aging. As in differentiated cells, hypermethylated sequences were enriched in chromatin repressive marks. Most importantly, hypomethylated CpG sites were strongly enriched in the active chromatin mark H3K4me1 in stem and differentiated cells, suggesting this is a cell type-independent chromatin signature of DNA hypomethylation during aging. Analysis of scedasticity showed that interindividual variability of DNA methylation increased during aging in MSCs and differentiated cells, providing a new avenue for the identification of DNA methylation changes over time. DNA methylation profiling of genetically identical individuals showed that both the tendency of DNA methylation changes and scedasticity depended on non-genetic as well as genetic factors. Our results indicate that the dynamics of DNA methylation during aging depend on a complex mixture of factors that include the DNA sequence, cell type and chromatin context involved, and that, depending on the locus, the changes can be modulated by genetic and/or external factors.

Introduction

Genomic DNA methylation is known to change during lifetime and aging (Jaenisch and Bird 2003). Some changes play important roles in development but others occur stochastically without any apparent biological purpose (Fraga 2009; Feil and Fraga 2012). These molecular alterations, which are known as the epigenetic drift, are currently being investigated as they have been proposed to account for many age-related diseases (Bjornsson *et al.* 2004; Heyn *et al.* 2013; Timp and Feinberg 2013). Various recent studies using 1.5K and 27K Illumina methylation arrays have identified a group of gene promoters in blood that become hypermethylated during aging (Christensen *et al.* 2009; Rakyan *et al.* 2010; Teschendorff *et al.* 2010; Bell *et al.* 2012; Fernandez *et al.* 2012). Interestingly, some of these studies have also shown that these DNA sequences are enriched in bivalent chromatin domains in embryonic stem cells (Rakyan *et al.* 2010; Fernandez *et al.* 2012; Heyn *et al.* 2012) and repressive histone marks such as H3K9me3 and H3K27me3 in differentiated cells (Rakyan *et al.* 2010), and that many of them are also frequently hypermethylated in cancer. However, drawing conclusions from some of these studies is limited by their low genome coverage (less than 0.1%) and the location of the sequences analyzed (mainly at gene promoters). Further studies using HumanMethylation450 BeadChip and larger cohorts (Heyn *et al.* 2012; Hannum *et al.* 2013; Johansson *et al.* 2013) have, though, corroborated most of the previous observations with the 27K methylation arrays and have, in addition, identified new sets of genes that become hypermethylated and hypomethylated during aging in humans. Finally, a recent study that analyzed the genome wide DNA methylation status of newborns, middle-aged individuals and centenarians confirmed the results obtained with the methylation arrays and showed that aging is associated with overall hypomethylation, which primarily occurs at repetitive DNA sequences (Heyn *et al.* 2012). Most of the above studies were conducted with whole blood and, consequently, changes in cell heterogeneity during aging could have affected the results (Calvanese *et al.* 2012; Houseman *et al.* 2012). However, some genes presented consistent changes in different tissues which indicates that, in some cases, the changes truly are associated with aging (Rakyan *et al.* 2010; Horvath *et al.* 2012). Interestingly, Houseman and colleagues (Houseman *et al.* 2012) have recently reported an algorithm that, using the DNA methylation values of certain genes, estimates the relative proportion of the different blood cell types in a specific sample. This algorithm was successfully used by

Liu and colleagues in a study to identify DNA methylation alterations associated with rheumatoid arthritis (Liu *et al.* 2013).

In addition to the studies using blood, other works have identified specific DNA methylation signatures of aging in differentiated cell types including brain (Hernandez *et al.* 2011; Numata *et al.* 2012; Guintivano *et al.* 2013; Lister *et al.* 2013), muscle (Zykovich *et al.* 2014) and saliva (Bocklandt *et al.* 2011). Two studies have analyzed DNA methylation during aging in human adult stem cells: Bork and colleagues (Bork *et al.* 2010) used 27k methylation arrays to analyze the DNA methylation status of mesenchymal stem cells (MSCs) obtained from young (21–50 years) and old donors (53–85 years) and found similar DNA methylation changes over time during prolonged *in vitro* culture and *in vivo* aging. Using the same methylation arrays, Bocker and colleagues (Bocker *et al.* 2011) observed a bimodal pattern of methylation changes in older hematopoietic progenitor cells, with hypomethylation of differentiation-associated genes, as well as *de novo* methylation events resembling epigenetic mutations. Recent studies in mice have revealed a number of genome-wide alterations in DNA methylation (Taiwo *et al.* 2013) which might play an important role in the functional decline of hematopoietic stem cells during aging (Beerman *et al.* 2013). To study the role of DNA methylation in adult stem cell aging further, the present study used HumanMethylation450 BeadChips to characterize the genome wide DNA methylation status of bone marrow MSCs obtained from individuals aged between 2 and 92. We then systematically compared our results with previously published data to identify the chromatin signatures associated with DNA methylation changes in adult stem cells and to determine whether these changes were also present in other tissues. Finally, we analyzed monozygotic twins of different ages to determine the effect of genetic factors on the DNA methylation changes during aging identified in our study.

Results

Global DNA methylation profiling in adult MSCs

To identify DNA methylation changes during MSC aging we compared the DNA methylation status of 429789 CpG sites in 34 independently isolated primary MSC, obtained from individuals from 2 to 92-years old, using the HumanMethylation450 BeadChip (Illumina®) (**Supplemental Fig. S1 and Supplemental Table 1**).

Using an empirical Bayes moderated t-test (see Materials and Methods) we first identified 64142 autosomal CpG sites which were differentially methylated (dmCpGs) (FDR<0.05) between MSCs obtained from young (ages ranging from 2 to 22) and elderly (aged between 61 and 91) individuals. Hierarchical clustering of all samples using the dmCpGs alone enabled each sample to be correctly allocated to its corresponding age group (**Figure 1A**). Of the dmCpG sites, 18735 (29.20%) had become hypermethylated and 45407 (70.80%) hypomethylated with aging (**Figure 1B and Supplemental Tables 2, 3)**.

To study, from a functional genomics point of view, the characteristics of these dmCpG sites we first determined their distribution within the different regions of the CpG islands (Wu *et al.* 2010). Interestingly, both hyper- and hypomethylated CpG sites were enriched in non CpG islands (CGI) (chi-square test; $p<0.001$, OR=2.58 and $p<0.001$, OR=1.76 respectively) (**Figure 1C**) and in intragenic DNA regions (chi-square test; $p<0.001$, OR=1.23 and $p<0.001$, OR=1.34 respectively) (**Figure 1D**).

To validate the results obtained with the methylation arrays, we randomly selected 5 of the sequences previously identified and analyzed their methylation status by bisulfite pyrosequencing in an independent cohort of 46 MSCs obtained from individuals from 7 months to 80-years old (**Supplemental Table 1).** In total, in the validation phase we obtained information on the DNA methylation status of 950 CpGs. The sequences selected corresponded to the genes *HAND2* and *SIX2,* which become hypermethylated with aging, and to the genes *TBX15*, *PITX2* and *HOXA11*, which become hypomethylated. Bisulfite pyrosequencing results showed that all the sequences selected for validation displayed the same DNA methylation dynamics during aging as in the study samples (**Figure 1 E**).

Tissue-specific DNA methylation changes during aging

Global DNA methylation patterns are tissue/cell type-specific (Calvanese *et al.* 2012). To determine whether the CpG sites displaying DNA methylation changes during aging in adult stem cells are also affected in differentiated tissues, we used the same workflow described in the previous section to analyze the data obtained in previous aging studies which used the same methylation arrays with samples from blood (human whole blood from a mixed population of 426 Caucasian and 230 Hispanic individuals, with ages ranging from 19 to 101) and brain (neuronal and glial cells, from post mortem frontal cortex of 29 healthy individuals (14 male, 15 female, aged 32.6 ± 16.1) (Guintivano *et al.* 2013; Hannum *et al.* 2013) (**Supplemental Fig. S1**). To reduce confounding factors in the blood dataset, we first corrected for cellular heterogeneity with respect to the major cell subtypes (Houseman *et al.* 2012) to filter out only those associations which were the consequence of aging. Using this approach we identified 63512 hypermethylated and 60155 hypomethylated sequences in blood (FDR<0.05), 11603 hypermethylated and 14143 hypomethylated sequences in glial cells (FDR<0.05) and 5171 hypermethylated and 2380 hypomethylated sequences in neural cells (FDR<0.05) (**Supplemental Fig. S2 and Supplemental Tables 4, 5)**. As in MSCs, hypomethylated cytosines in the differentiated cells preferentially occurred at both non-CGI regions (chi-square test; blood, p<0.001, OR=2.35; neural, p<0.001, OR=1.74; glial, p<0.001, OR=3.03) and at intragenic regions (chi-square test; blood, p<0.001, OR=1.11; neural, p<0.001, OR=2; glial, p<0.001, OR=1.89) (**Supplemental Fig. S2**). However, in brain samples (neuronal and glial cells), hypermethylated cytosines occurred preferentially at both non-CGI regions (chi-square test; neural, p<0.001, OR=1.43; glial, p<0.001, OR=1.43) and at intragenic regions (chi-square test; neural, p<0.001, OR=1.1; glial, p<0.001, OR=1.1), while they occurred preferentially in both CGIs (chi-square test; p<0.001, OR=3.5) and at promoter regions (chi-square test; p<0.001, OR=1.49) in blood samples (**Supplemental Fig. S2**).

To identify possible cell type-independent DNA methylation signatures of aging, we created two additional datasets containing the hyper- and hypomethylated probes from selected subsets of the different tissues analyzed (**Figure 1F**). This approach showed only a small overlap between MSC and differentiated cells (42 hypomethylated and 38 hypermethylated), suggesting that systemic DNA methylation changes during aging are restricted to specific regions of the genome (**Figure 1F and Supplemental Tables 6, 7)**.

Hypermethylated CpG sites during aging are associated with repressive chromatin marks

In blood, DNA hypermethylation during aging has been shown to occur at gene promoters enriched in repressive histone marks such as H3K9me3 and H3K27me3 (Rakyan *et al.* 2010). To identify possible chromatin signatures associated with DNA hypermethylation during aging in adult MSCs, we compared our methylation data with previously published data on a range of histone modifications and chromatin modifiers in 10 different cell types obtained from healthy individuals (see Materials and Methods). In the present study we found statistically significant associations with the repressive histone marks H3K9me3, H3K27me3 and EZH2 in most differentiated ENCODE cell lines (Fisher´s exact test; $p<0.001$) (**Figure 2**), which is in line with previously published data (Rakyan *et al.* 2010). To determine whether these observations can be extrapolated to other cell types, we used the same approach to analyze the CpG sites which are hypermethylated during aging in blood, neural and glial cells (Guintivano *et al.* 2013; Hannum *et al.* 2013) (**Supplemental Table 4**). The results showed that hypermethylated CpG sites in blood and brain were enriched in the same chromatin marks identified in the adult MSCs (**Figure 2**), suggesting that chromatin context is an important cell type-independent mark of DNA hypermethylation during aging. Analysis of the 38 commonly hypermethylated CpG sites in blood, MSCs and neural and glial cells also showed statistically significant associations (FDR<0.05) with the repressive histone marks H3K9me3, H3K27me3 and EZH2 found in some types of differentiated cells (**Figure 2**).

DNA hypomethylation during aging preferentially occurs at H3K4me1 rich sites

To identify chromatin marks associated with CpG sites hypomethylated in aged MSCs, we aligned the DNA sequences identified in our study with the same database of histone modifications and chromatin modifiers described in the previous section. Of note is the fact that hypomethylation largely occurred at regions occupied by the active histone mark H3K4me1 in most of the ENCODE cell lines (FDR<0.05) (**Figure 2**).

To determine whether these associations occurred in differentiated cells, we used the same approach to analyze CpG hypomethylation during aging in blood, neural and glial cells (Guintivano *et al.* 2013; Hannum *et al.* 2013) (**Supplemental Table 5**). Blood and

brain samples showed similar enrichment patterns to those of the MSCs in that hypomethylated CpG sites were preferentially located at regions enriched in H3K4me1 (**Figure 2**). Interestingly, the analysis of the 42 commonly hypomethylated CpG sites in blood, MSCs and neural and glial cells only showed statistically significant associations with H3K4me1 (FDR<0.05) (**Figure 2A**).

Dynamics of interindividual DNA methylation variability during aging

As in most previous studies on DNA methylation and aging, our analytical design allowed the identification of DNA sequences showing a specific tendency to change (hyper- or hypomethylation) during aging, but not other putative DNA regions exhibiting no change tendency (i.e., sequences that do not become hyper- or hypomethylated with aging but rather show an increase or a decrease in interindividual variability). To address this issue, we carried out an alternative data analysis on our MSCs based on the aging-dependent behavior of interindividual variability (i.e. DNA methylation scedasticity). Interindividual variability was higher in MSCs obtained from older individuals than in those obtained from younger individuals (Figure 3A). Analysis of the scedasticity identified 16243 heteroscedastic CpG sites, of which 2437 were convergent and 13806 divergent. We also identified 124611 homoscedastic CpG sites, 68927 showing low interindividual variability in both young and old individuals (LV) and 55684 showing high interindividual variation in both populations (HV) (see Materials and Methods) (**Figure 3B, C and Supplemental Tables 8-11)**.

We studied these sequences from a functional genomics standpoint to identify factors associated with the behavior of DNA methylation changes during aging. We observed that divergent and HV CpG sites were preferentially enriched in non-CGIs (chi-square test; $p<0.001$, OR=1.59 and $p<0.001$, OR=1.58 respectively), and convergent and LV CpG sites in CGIs (chi-square test; $p<0.001$, OR=1.11 and $p<0.001$, OR=5.00 respectively) (**Figure 3D**). Both divergent and convergent sequences were more abundant in intragenic regions (chi-square test; $p<0.001$, OR=1.38 and $p<0.001$, OR=1.16 respectively), with HV being more frequently found in intergenic regions (chi-square test; $p<0.001$, OR=1.50), and LV in promoter regions (chi-square test; $p<0.001$, OR=3.62) (**Figure 3D**).

To determine whether scedasticity behavior can also identify DNA methylation changes during aging in differentiated cells we repeated these same analyses on previously

published blood DNA methylation data (Hannum *et al.* 2013). As Hannum *et al.*'s cohort contains DNA methylation data on more than 600 individuals, statistical analyses were carried out using a Brown-Forsythe test (see Materials and Methods). To discount a possible confounding effect of cell heterogeneity in the analysis of the scedasticity in blood, in addition to applying the algorithm described by Houseman et al. (Houseman *et al.* 2012), we carried out in silico functional analysis of the groups of genes established according to the behavior of the variance (see Materials and Methods). These analyses showed no significant associations between these groups of genes and any of the blood cell lineages examined (**Supplemental Tables 12 and 13**). As in MSCs, interindividual variability was higher in blood obtained from older individuals than in blood obtained from younger individuals (**Figure 4A**). Furthermore, in line with the findings for adult MSCs, in differentiated cells, the analyses identified 19454 heteroscedastic CpG sites, of which 4037 were convergent and 15417 divergent. Of the homoscedastic CpG sites, 92074 showed LV in both young and old individuals and 92753 showed HV in both populations (**Figure 4B, C**).

The role of genetic factors on DNA methylation changes during aging

To study the role of genetic factors on DNA methylation changes during aging we used HumanMethylation450 BeadChips to analyze the DNA methylation status of 24 monozygotic twins from two age groups (young, 21-22-yo and old, 58-66-yo). The effect of genotype was assessed comparing the Euclidean distance (ED) and the interindividual variability in methylation values between old and young monozygotic (MZ) pairs. To reduce possible bias due to cell heterogeneity, DNA methylation data was corrected with the algorithm described by Houseman (Houseman *et al.* 2012). As in the larger cohort previously analyzed (**Figure 4**), interindividual DNA methylation variability substantially increased during aging in the MZ twins (**Figure 5A**). Interestingly, mean ED between MZ twins also increased (> 2-fold) with age in 46763 CpG sites (**Figure 5B and Supplemental Table 14)**, which indicates that, at these CpG sites, the increase in interindividual methylation variability depends, at least in part, on non-genetic factors. In 24782 of these sequences **(Figure 5B and Supplemental Table 15)** the increase in ED (> 2-fold) was higher than could be accounted for solely by interindividual variability, suggesting that, in these CpG sites, genetic factors play a less important role in the regulation of DNA methylation changes during aging. However, in

21908 of these sequences **(Figure 5B and Supplemental Table 16)**, the increase in ED (> 2-fold) was less than could be accounted for solely by interindividual variability, which suggests that, in contrast, at these CpG sites, genetic factors are more relevant for the regulation of DNA methylation during aging.

Although the general trend was an increase in ED with age, for 22542 CpG sites ED between older MZ pairs decreased (> 2-fold) (**Figure 5B and Supplemental Table 17).** As the EDs between older MZ individuals are greater than those between younger MZs in more than half the sequences identified, our results support the notion that, in general, DNA methylation patterns diverge with age, even in genetically identical individuals. In 11624 sequences **(Figure 5B and Supplemental Table 18)** the decrease in ED (> 2-fold) was lower than could be accounted for solely by interindividual variability, which suggests that, in these CpG sites, genetic factors play a more important role in the regulation of DNA methylation changes during aging. In 10883 sequences **(Figure 5B and Supplemental Table 19)**, the decrease in ED was higher than could be accounted for solely by interindividual variability, indicating that in these CpG sites, genetic factors play a less important role in the regulation of DNA methylation during aging. As in the analysis of the previously published blood DNA methylation data, in silico functional analysis of the groups of genes identified in the monozygotic twins (**Supplemental Tables 20,21**), suggested that, after correcting with the Houseman algorithm, cell heterogeneity had little impact on the Euclidean distances for changes in DNA methylation with age.

Comparative analysis of the interindividual variation and the EDs suggests that the effect of genotype on the regulation of DNA methylation changes during aging was locus-specific. Thus, to identify those DNA regions differentially affected by the genotype, we used Circos representations to study the genomic distribution of CpG sites which showed changes in ED with age (**Figure 5C**). The results demonstrated that whilst CpG sites showing a decrease, or no difference, in ED between young and old MZs presented a random distribution, those showing an age-dependent increase in ED were strongly enriched in subtelomeric DNA regions. The greatest changes occurred at chromosomes 11 and 19 and, in general, clustering occurred at the same genomic regions in both young and old twins.

To study the effect of the genotype on DNA methylation and its interindividual variability during aging we analyzed the Twins data using similar strategies to those

described in previous sections, identifying 41987 hypermethylated, 56923 hypomethylated, 1018 convergent, 1635 divergent, 58680 HV and 59795 LV CpG sites (data not shown). The comparison of EDs between young and old MZ pairs for these groups of genes showed that the effect of genotype depended on the tendency and the scedasticity of the change (**Figure 5D**).

ED increased (>2-fold) with age in 9.5% of the hypomethylated and in 14% of the hypermethylated CpGs, suggesting that genetic factors have a greater effect on the former during aging **(Figure 5D and Supplemental Tables 22, 23)**. ED increased (>2-fold) in most (83.73%) of the divergent CpG sites and decreased (>2-fold) in most (66.7%) of the convergent CpG sites **(Figure 5D and Supplemental Tables 24, 25)**. However, changes in interindividual variability were higher than the increase or decrease in ED **(Figure 5D)**, which indicates that genetic factors play a role in the regulation of DNA methylation of these DNA regions during aging. Interestingly, ED also increased in most of the HV and LV sequences (>2-fold) during aging **(Figure 5D).** Furthermore, in most CpG sites, the increase in ED between the MZ twins was higher than the interindividual variability changes during aging **(Figure 5D)**, suggesting that genotype has little effect on epigenetic drift in homoscedastic DNA regions.

Discussion

Recent studies have shown that DNA methylation is altered during aging in a number of differentiated cell types (Rakyan *et al.* 2010; Teschendorff *et al.* 2010; Bell *et al.* 2012; Fernandez *et al.* 2012; Heyn *et al.* 2012; Numata *et al.* 2012; Guintivano *et al.* 2013; Hannum *et al.* 2013; Johansson *et al.* 2013). Here, we studied the dynamics and the context of DNA methylation changes during aging in human adult stem cells as they have been proposed to play an important role in aging (Sharpless and DePinho 2004). Indeed, a recent study in mice showed that epigenomic alterations of the DNA methylation landscape contribute to the functional decline of hematopoietic stem cells (HSCs) during aging (Beerman *et al.* 2013). To analyze our DNA methylation data, we first used an analytical strategy similar to that used in most of the previous studies on DNA methylation and aging (i.e. linear models). Using this approach, we identified 18735 CpG sites which were hypermethyated and 45407 which were hypomethylated during aging in MSCs, which provides support for the idea that, as in blood (Heyn *et al.* 2012), aging is associated with global DNA hypomethylation in MSCs. In addition, we validated 5 of the genes identified through the methylation arrays (*HAND2*, *SIX2*, *TBX15*, *PITX2*, and *HOXA11*) by bisulfite pyrosequencing, using an independent sample set of 46 MSCs obtained from individuals from 7 months to 80-years old. The results corroborated the data obtained from the methylation arrays and suggest that our genome-wide data can be extrapolated to independent sample sets of MSCs. *HAND2* and *SIX2* genes code for transcription factors and have been also found hypermethylated in several cancer types (Rauch *et al.* 2006; Tong *et al.* 2010; Jones *et al.* 2013). In contrast, the genes which are hypomethylated during MSC aging, *TBX15*, *PITX2*, and *HOXA11*, code for transcription factors involved in several differentiation and developmental processes (Singh *et al.* 2005; Gross *et al.* 2012; Gage *et al.* 2014).

Interestingly, 80 of the differentially methylated sequences identified in the MSCs were present in both blood and brain, which is in line with previous observations that suggest the existence of systemic DNA methylation changes during aging (Rakyan *et al.* 2010; Heyn *et al.* 2012). However, as many of the sequences were not common to different tissues, our data indicate that, as has recently been proposed (Christensen *et al.* 2009; Day *et al.* 2013) systemic changes are restricted to specific loci, and cell type plays an important role in the regulation of DNA methylation changes over time.

The factors determining the behavior of DNA methylation during aging have received much attention during the last few years. Recent works have shown that genes which are hypermethylated in blood during aging are associated with the presence of bivalent chromatin domains in embryonic stem cells (Rakyan *et al.* 2010; Teschendorff *et al.* 2010; Fernandez *et al.* 2012; Heyn *et al.* 2012) and with repressive histone marks (H3K27me3/H3K9me3) in differentiated cells (Rakyan *et al.* 2010). Our data indicate that the same repressive histone marks in differentiated cells are also present in sequences in those MSCs which are hypermethylated during aging, implying that, independent of morphogenic potential and/or cell type, these repressive histone marks are associated with DNA methylation gain during aging. Of note, our data provide new evidence that sequences which are hypomethylated in MSCs and differentiated cells during aging are strongly enriched in the active chromatin mark H3K4me1, which suggests that this histone modification is a cell type-independent chromatin signature of DNA hypomethylation during aging. Interestingly, H3K4me1 has recently been associated with enhancers (Rada-Iglesias *et al.* 2010), genomic regions that play a fundamental role in cis-regulation of gene function. In addition, a recent study has shown that DNA hypomethylation within specific transposable elements is associated with tissue-specific enhancer marks, including H3K4me1, suggesting that these sequences might play an important role in tissue-specific epigenetic gene regulation (Xie *et al.* 2013), which implies that H3K4me1-associated DNA hypomethylation could play a role in the deregulation of gene expression during aging (Bahar *et al.* 2006). Further parallel studies analysing DNA hypomethylation in enhancers and gene expression during aging should shed light on this matter. Collectively, our data indicate that, although there are few altered DNA sequences which are common to different cell types, the chromatin signatures associated with DNA hyper- and hypomethylation during aging were similar for different tissues, supporting the notion that chromatin context is associated with the dynamics of systemic DNA methylation changes during aging. The reasons why the repressive histone marks H3K27me3/H3K9me3 favor hypermethylation and the active histone mark H3K4me1 promotes hypomethylation during aging are not known. A simple explanation could be the preferential location of DNA methyltransferases (DNMTs) at repressive chromatin regions (Jeong *et al.* 2009). Repressive chromatin regions could be predisposed to becoming hypermethylated due to the abundance of DNMTs. In contrast, active chromatin regions would be more

susceptible to losing methylation because the low levels of DNMTs at these regions make it more difficult to maintain DNA methylation patterns after mitosis. This possibility is supported by the fact that postmitotic tissues such as brain (Numata *et al.* 2012; Guintivano *et al.* 2013) and muscle (Zykovich *et al.* 2014) present far fewer hypomethylated sequences during aging than highly mitotic cells such as blood and MSCs. Further studies analyzing the genome wide distribution of DNMTs during aging are needed to support this possibility.

One possible limitation of our study is the purification and the *in vitro* culture of MSCs (Calvanese *et al.* 2008; Choi *et al.* 2012), although this should have no great impact when comparing young and old MSCs as both sets of samples were cultured under exactly the same conditions. Moreover, cell heterogeneity, which is a major issue in DNA methylation studies (Houseman *et al.* 2012; Guintivano *et al.* 2013), has less impact in relation to MSCs as they are more homogeneous than blood cell populations. However, to minimise the impact of cell heterogeneity in our analysis of blood we corrected DNA methylation data with a recently published algorithm (Houseman *et al.* 2012), which yielded slightly different sequences to those previously proposed, suggesting that some of the DNA changes previously identified might be cell-type dependent. However, as this algorithm considers only the major cell subtypes, possible variations driven by minor subtypes would not be detected. Another limitation of our study is that the differences in the number of individuals analyzed and different data analyses undertaken make difficult the interpretation of the comparison of age-dependent DNA methylation changes in different cell types. However, the conserved pattern of chromatin signatures in stem and differentiated cells suggests that H3K9me3/H3K27me3 and H3K4me1 are truly tissue-independent histone marks of DNA hyper- and hypomethylation respectively during aging.

As in most previous studies on DNA methylation and aging, CpG sites showing DNA methylation changes during lifetime associated with a specific tendency (i.e. hyper- or hypomethylation) were identified. However, using this analytical approach means that other possible changes occurring at CpG sites displaying high interindividual variability in both young and old individuals and/or age-dependent interindividual variability are overlooked. To address this issue, we re-analyzed the DNA methylation data to characterize the age-dependent interindividual variability (i.e. scedasticity).

Using this approach we identified 16243 heteroscedastic (2437 convergent and 13806 divergent), and 55684 homoscedastic CpG sites with high (HV) and 68927 with low (LV) interindividual variability. Most of these CpG sites were not identified through linear model analysis, leading us to suggest that DNA methylation changes during aging might be more frequent than has previously been thought. Interestingly, although there were some CpG sites that converged during aging, most of the heteroscedastic changes were divergent, providing support for the notion that interindividual DNA methylation variability increases during lifetime (Gemma *et al.* 2013; Ong and Holbrook 2013). Although the behavior adults stem cell populations during aging is still poorly understood (Pollina and Brunet 2011), the clonal expansion or decline of specific cell populations could affect the interpretation of changes of interindividual DNA methylation variability with aging. As it has been proposed that the number of MSCs declines with age (Stolzing *et al*. 2008), it is possible that the increase in interindividual variability might in fact be even larger than was observed in our study.

Functional genomics analyses of the groups of CpG sites established according to the behavior of the variance revealed that low variable CpG sites were enriched in CpG islands and gene promoters. As DNA methylation occurring at CpG island promoters has been proposed to play an important role in gene regulation (Bird 1986; Bird and Wolffe 1999; Calvanese *et al.* 2012), our results could indicate that the DNA methylation involved in gene regulation is protected against the stochastic epigenetic changes that occur during lifetime (Feil and Fraga 2012). Interestingly, analysis of the interindividual variability of DNA methylation during aging in blood, showed that, as in adult stem cells, the DNA methylation patterns of differentiated cells also diverge with age, thereby supporting the notion that a systemic epigenetic drift occurs during the lifetime of higher organisms (Feil and Fraga 2012; Issa 2014). To confirm that the sequences identified in blood after correcting with the Houseman algorithm were not affected by cell heterogeneity, we carried out in silico functional analysis to discard a possible blood cell lineage-dependent regulation. The analyses showed no meaningful associations, which further supports our contention that, after correcting with the Houseman algorithm, cell heterogeneity had a minor impact on our blood DNA methylation data.

Previous reports have demonstrated that genetic factors play an important role in the regulation of DNA methylation during aging (Heijmans *et al.* 2007; Coolen *et al.* 2011; Gertz *et al.* 2011; Bell *et al.* 2012). To determine whether the effect of genotype is different depending on the intrinsic behavior of the DNA changes during aging at each specific CpG site, we analyzed the DNA methylation status of monozygotic twins of different ages. The results showed that interindividual variability increased with aging, in agreement with the notion that epigenetic drift during lifetime occurs even in genetically identical individuals (Fraga *et al.* 2005; Wong *et al.* 2010; Pirazzini *et al.* 2012; Talens *et al.* 2012; van Dongen *et al.* 2012). However, our results also showed that the DNA methylation status of some CpG sites may converge during lifetime. Specifically, the analysis of genetically identical individuals revealed that the effect of genotype depended on the intrinsic behavior of the DNA methylation changes during aging. For example, although the mechanisms underlying methylation convergence are still largely unknown, our MZ data indicate that genetic factors must be involved, at least in part, as the intrapair changes were similar to, or even less than, the interindividual variations. In addition, in contrast to the convergent and divergent CpG sites, genotype seems to play a less important role in whether the CpG sites display high or low interindividual variability, as evidenced by the fact that the increase in ED in the homoscedastic sequences for MZ twin pairs during aging was higher than the differences explained by interindividual variability. Of particular note is the finding that genotype had the lowest effect on the CpG sites, displaying high interindividual variability in young and old individuals, evidenced by the increase Euclidean distance in MZ twins during aging being similar to or even higher than the increase in interindividual variability. Our results indicate that these CpG sites, which have received little attention until now, might be important targets of environmental and/or stochastic epigenetic variation during development and aging. Although we have reduced the effect of cell heterogeneity and immune status over time (Allegretta *et al.* 1990) using the Houseman algorithm (Houseman *et al.* 2012) and by performing several functional in silico analyses of the groups of the genes showing age-related changes in Euclidean distance, we cannot completely discount a partial effect of these in our results.

Our data indicate that the differences in the effect of genotype on DNA changes during lifetime depend largely on the genomic region involved, which is in agreement with

previously published data (Wong *et al.* 2010). In line with this, the greatest DNA methylation changes for MZs were clustered at subtelomeric DNA regions, which suggests that the regulation of DNA methylation at these sequences is largely independent of genetic factors. Interestingly, subtelomeric DNA methylation has been shown to be affected by environmental factors (unpublished observations). It is worth noting that, although for most CpG sites the ED in young twins was lower than for older twins, they still clustered in the same subtelomeric regions, providing support for the previous proposal that epigenetic drift starts early in life (Martino *et al.*; Kaminsky *et al.* 2009; Ollikainen *et al.* 2010; Wong *et al.* 2010) and accumulates during lifetime at particular CpG sites that, for still unknown reasons, evade the control of genetic factors (Fraga 2009).

Collectively, our results indicate that the dynamics of DNA methylation during lifetime in humans is associated with a complex mixture of factors. These include the DNA sequence itself, tissue type and, in particular the chromatin context, where repressive histone modifications such us H3K9me3 and H3K27me3 are related to DNA hypermethylation and, most notably, the active histone mark H3K4me1 is related to DNA hypomethylation. Finally, depending on the locus, the changes appear to be modulated by genetic and/or external factors.

Materials and methods

Isolation and culture of MSCs

MSCs were purchased from Lonza (Verviers, Belgium), Millipore (Billerica, MA, USA), and Inbiobank. (San Sebastian, Spain) or directly obtained from young and elderly donors. After informed consent, bone marrow aspirates were obtained from one group of patients and, from a second group, bone scrapings were obtained following hip replacement surgery. Mononuclear cells were isolated by Ficoll density centrifugation (400 g, 25 min, 20C), washed twice by sedimentation with phosphate buffer (300 g, 5 min) and the cells resuspended in MSC medium (DMEM plus 10% FBS) and seeded into culture flasks (Nunc, Roskilde, Denmark) at 1.5x10e5 cells/cm^2 and allowed to adhere for 24 hours. MSCs were then cultured (37C, 5% CO_2) in MSC medium. DNA methylation analyses were carried out at cell passages 4-6 (**Supplemental Table 1**).

MZ twins samples

Genomic DNA from 24 samples from the Italian Twin Registry, corresponding to 12 pairs of MZ twins, were extracted from buffy coats following standard procedures. Two different age groups were included for array-based DNA methylation profiling; one included individuals between 21 and 22 years old (*young* MZ twins), and the other individuals between 58 and 66 (*old* MZ twins). The sample distribution by gender was the same in both groups.

Genome-wide DNA methylation analysis with high-density arrays

Microarray-based DNA methylation profiling was performed with the HumanMethylation450 BeadChip (Bibikova *et al.* 2011). Bisulfite conversion of DNA was performed using the EZ DNA Methylation Kit (Zymo Research, Orange, CA) following the manufacturer's procedures, with the modifications described in the Infinium Assay Methylation Protocol Guide. Processed DNA samples were then hybridized to the BeadChip (Illumina), following the Illumina Infinium HD Methylation Protocol. Genotyping services were provided by the Spanish "Centro Nacional de Genotipado" (CEGEN-ISCIII)" (www.cegen.org).

Datasets of blood and brain samples

DNA methylation data of blood (Hannum *et al.* 2013) and brain (neuron and glia) (Guintivano *et al.* 2013) samples produced with the HumanMethylation450 BeadChip were used to compare with the results obtained in MSCs. DNA methylation β value data was downloaded from GEO accession numbers GSE40279 and GSE41826. The data

analysis workflow is outlined in **Supplemental Fig. S1.**

HumanMethylation450 BeadChip data preprocessing

IDAT files from the HumanMethylation450 BeadChip were processed further using the R/Bioconductor package *minfi* (Hansen and Aryee). In order to adjust for the different probe design types present in the HumanMethylation450 BeadChip architecture, red and green signals from the IDAT files were corrected using the SWAN algorithm (Makismovic *et al.* 2012). No background correction or control probe normalization was applied. Probes where at least two samples had detection p-values over 0.01 were filtered out. In accordance with Du *et al.* (Du *et al.* 2010), both beta values and m-values were computed and employed across the analysis pipeline. M-values were used for all the statistical analyses, assuming homoscedasticity (with the exception of the blood heterogeneity adjustment), while beta values were mostly used for the intuitive interpretation and visualization of results.

Filtering confounding probes

Probes located in the X/Y chromosomes were removed from the dataset when differential methylation profiles were analyzed. Probes that had been found to cohybridate with probes in the sex chromosomes (Lemire *et al.* 2013) were also removed. We used the information from the SNP137Common track from the UCSC Genome Browser (Sherry *et al.* 2001) in order to remove those probes with an SNP located inside their 2bp central region.

Batch effect correction

Multidimensional Scaling (MDS) was employed to detect whether there was any significant batch effect depending on the different HumanMethylation450 BeadChip plates which comprised the experiments. When there was, the ComBat method implemented in the R/Bioconductor package *sva* (Leek *et al.*) was used to adjust the datasets accordingly, employing the variable *age* as the outcome of interest and the sample plate as a batch covariate.

White blood cell heterogeneity adjustment

Methylation data for the Blood and Twins datasets was adjusted for blood cell heterogeneity, with respect to the major cell subtypes, using the method described in Houseman et. al. (Houseman *et al.* 2012). In order to feed this method, we used the original 27k database of purified white blood cell subtypes included in the original implementation of the algorithm. The correction was performed on the beta values due

to the fact that the 27k database was expressed using those units. M-values were obtained from the corrected beta values for subsequent downstream analyses.

Detection of differentially methylated probes

For the MSC dataset, the 34 samples were divided into two groups: *young* (ages ranging from 2 to 22) and *old (*ages between 61 and 92). Similarly, samples in the Twins dataset were divided into *young* (ages ranging from 21 to 22) and *old* (age between 58 and 66). For the neuron and glia datasets, the two groups were defined by taking those individuals whose age was below the 33rd percentile (*young*) and above the 66th percentile (*old*). Blood samples were not divided into groups, and the age predictor was used as a quantitative covariate. For the MSCs, Twins, neuron and glia datasets, significant methylation of a probe was determined by the moderated t-test implemented in the R/Bioconductor package *limma* (Smyth 2005). Probes in the blood dataset were tested with a linear regression. A linear model, with methylation level as response and *age* as the only predictor, was used on all the datasets. P-values were corrected for multiple testing using the Benjamini-Hochberg method for controlling the false discovery rate (FDR). A significance level of 0.05 was employed to determine differentially methylated probes. An additional threshold of effect size was applied, meaning that only those probes with the strongest differences between groups (the top 70%) were selected. The application of this threshold is essential to remove those differences prone to coming from technical artifacts, and consequently ensure a more biologically sound statistical data analysis (Pan *et al*. 2005). Our threshold was adjusted according to the differences in M-values between groups in the brain and MSC datasets and the slope coefficients extracted from the blood dataset linear regression model.

Analysis of variability trends

To analyze aging-dependent behavior of DNA interindividual variability (i.e. DNA methylation scedasticity), two groups, corresponding to *young* (samples where *age* was below the 33rd percentile) and *old* (those where *age* is above the 66th percentile) individuals, were selected for all the datasets. This separation allows the method to focus on the global tendency of the variability, and be less dependent on a fixed, underlying model. A Brown-Forsythe test for the equality of variances was used to determine which probes in the blood dataset had significantly different variability in methylation between the two groups. For the remaining datasets, and due to the small number of available samples and low statistical power for conducting a variance test, a

simple descriptive approach was used, labeling a probe as having a significant difference in methylation variability when the absolute value of the base-2 logarithm of the change of the variances for the two groups was greater than 3 fold. We did not apply any threshold of effect size for any of the datasets. For the blood dataset, p-values were corrected for multiple testing using FDR (Benjamini-Hochberg method) and a significance level of 0.05 used to determine which probes had a significant trend in variability. Two special subsets of probes with no significant trends in variability were generated: one, named HV (High Variance), for those probes with variance values above the 75th percentile of the whole set of variances for both the *young* and *old* sample groups, and one named LV (Low Variance), generated with those probes where both young and old variances were below the 25th percentile.

The *in silico* functional analysis and interpretation of the groups of genes established according to the behavior of the variance in blood was performed using the Database for Annotation, Visualization and Integrated Discovery (DAVID) and the "Gene ontology" and “UP_TISSUE" categories (Dennis *et al.* 2003; Huang da *et al.* 2009).

Measuring intra- and interindividual distance

Euclidean distances between twins were computed for every probe in the original Twins dataset, using beta-values. In a simple scenario, the Euclidean distance accounts for the absolute difference between the beta values of the two siblings. Differences in distances were computed as the base-2 logarithm of the fold change between the average Euclidean distance for the young and old sample groups.

Histone enrichment analysis

In order to analyze the enrichment of a histone mark on a given subset of probes, we used the information contained in the UCSC Genome Browser Broad Histone track from the ENCODE Project (Rosenbloom *et al.* 2010; Rosenbloom *et al.* 2012) **(Supplemental Table 26)**. Histone peak data for every histone modification and chromatin modifier in hESCs and 10 different cell types obtained from healthy individuals were downloaded from the UCSC Genome Browser. Small peaks were discarded when they were completely contained within wider peaks. Following the ENCODE Broad Histone Methods description, discrete intervals of ChIP-seq fragment enrichment were identified using Scripture, a scan statistics approach, under the assumption of uniform background signal (http://genome.ucsc.edu//cgi-bin/hgTrackUi?db=hg19&g=wgEncodeBroadHistone).

For each combination of cell line and mark, a 2x2 contingency table was built to determine its association with the input subset of probes. Probes in the array were classified according to whether they belonged to the subset or not, and whether they intersected with a significant broad peak for the given combination of cell line and mark. A Fisher´s exact test was used to determine if the given subset of probes was significantly enriched for each combination of cell line and mark. P-values were corrected for multiple testing using FDR (Benjamini-Hochberg method) and a significance level of 0.05 was used to determine which probes had significant enrichment. The base-2 logarithm of the Odds Ratio was used as a measure of effect size.

Genomic region analysis

The probes in the microarray were assigned a genomic region according to their position relative to the transcript information extracted from the R/Bioconductor package *TxDb.Hsapiens.UCSC.hg19.knownGene* (Carlson). A probe was said to be in a *Promoter* region if it was located inside the first exon, the 5'-UTR or a region up to 2kbp upstream of the transcription start site (TSS) of any given transcript. Similarly, a probe was labeled as *Intragenic* if it was inside any intron or any exon other than the first. *Intergenic* probes were determined as those not falling into either of the two previous categories. According to this definition, a probe could be in both a *Promoter* and an *Intragenic* region at the same time for different transcripts. A contingency table was built for each selected subset of probes and a given genomic region, with one variable indicating whether a given probe belonged or not to the subset, and the other indicating whether a given probe was labeled with the selected region. Significance of the association was determined by a Pearson's chi-squared test with Yates' continuity correction. A significance level of 0.05 was used to determine whether a subset was dependent with respect to a given genomic region. Odds Ratio was used as a measure of effect size.

CpG Island status analysis

The CpG island locations used in the analyses were obtained from the R/Bioconductor package *FDb.InfiniumMethylation.hg19* (Triche 2013) The generation procedure of these CpG Islands is described by Wu and colleagues (Wu *et al.* 2010). *CpG shores* were defined as the 2kbp regions flanking a CpG Island. *CpG shelves* were defined as the 2kbp region either upstream or downstream of each CpG shore. Probes not

belonging to any of the regions thus far mentioned were assigned to the special category *Non-CpG Island*. Each probe was assigned to only one of the categories. A 4x2 contingency table was constructed for every subset of probes in order to study the association between the given subset and the different CpG Island categories. A chi-squared test was used to determine if any of the categories had a significant association with the given subset. For each of the CpG Island status levels, a 2x2 contingency table was defined and another chi-squared test was used to independently evaluate the association of the given subset with each status level, a significance level of 0.05 being employed for all tests. Effect size was reported as the Odds Ratio for each of the individual tests.

Microarray background correction

Although it is sometimes referred to as a genome wide solution, the HumanMethylation450 BeadChip only covers a fraction of the entire genome. In its 27k predecessor, the probes were mainly located at gene promoter regions, while in addition to the promoter probes, the HumanMethylation450 BeadChip includes probes located inside genes and in intergenic regions (Dedeurwaerder *et al.* 2011).

The irregular distribution of probes can lead to unwanted biases when studying whether a selected subset of probes is enriched with respect to any functional or clinical mark. A reference to the background distribution of features was included in every type of statistical test performed in order to prevent our conclusions from being driven by the irregular distribution of probes. In qualitative tests (CpG Island status, genomic region or histone mark enrichment), the contingency matrix was built to represent the background distribution of the microarray. Thus, any significant result would indicate a departure from the fixed background distribution, and ignore any manufacturer bias.

Circos data track smoothing

In order to plot the CpG information on the Circos genome-wide graphs (Krzywinski *et al.* 2009), smoothing was applied to our data. Broad histone peak information from UCSC Genome Browser was averaged by partitioning the genome into intervals of 200kbp and assigning to each a score corresponding to the average of the broad peak scores found within it. CpG locations were not smoothed. Distances in the Twins dataset were averaged using a 2Mbp window size.

Bisulfite pyrosequencing

DNA methylation patterns of representative dmCpGs during aging were analyzed by

bisulfite pyrosequencing in an independent sample set of 46 MSCs obtained from individuals of different ages (**Supplemental Table 1**). Bisulfite modification of DNA was performed with the EZ DNA Methylation-Gold kit (Zymo Research) following the manufacturer's instructions. The set of primers for PCR amplification and sequencing were designed using the specific software PyroMark assay design (version 2.0.01.15). Primer sequences were designed to hybridize with CpG free sites to ensure methylation-independent amplification **(Supplemental Table 27)**. After PCR amplification of the region of interest with the specific primers, pyrosequencing was performed using PyroMark Q24 reagents, and vacuum prep workstation, equipment and software (Qiagen). A linear regression model was fitted to the pyrosequencing methylation data using *age* as a predictor.

Data analysis workflow

All the necessary steps for upstream and downstream analyses were defined and implemented using the Snakemake tool (Köster and Rahmann 2012). This tool helps data scientists to generate a reproducible and inherently parallel processing pipeline. The source code of the workflow is included as Supplemental Material.

Data access

The HumanMethylation450 BeadChip data sets from this study have been submitted to the NCBI Gene Expression Omnibus (GEO; http://www.ncbi.nlm.nih.gov/geo/) under accession number GSE52114 (SubSeries GSE52112 and GSE52113).

Acknowledgments

We thank Ronnie Lendrum for editorial assistance and Tim Triche, Jr. for his invaluable advice. This work has been financially supported by the Fondo de Investigaciones Sanitarias FIS/FEDER (PI11/01728 to AF.F., PI 12/0615 to J.A.R.; PI10/0449 to P.M, and PI11/0119 to C.B.); the ISCIII-Subdirección General de Evaluación y Fomento de la Investigación (Miguel Servet contract: CP11/00131 to A.F.F., and CP07/0059 to C.B.); the Spanish Ministry of Health (PS09/ 02454 and PI12/01080 to M.F.F.); the Spanish National Research Council (CSIC; 200820I172 to M.F.F.); IUOPA (to C.F. and G.F.B.); Fundacion Cientifica de la AECC (to R.G.U. and to P.M.); Fundación Ramón Areces (to M.F.F); and FICYT (to E.G.T.). J.G-C receives funding from the Fondo de Investigaciones Sanitarias (FIS; PI05/2217 and PI08/0029) and the Madrid Regional

Government (S-BIO-0204-2006 and S2010/BMD-2420). J.A.R. receives funding from the Fondo de Investigaciones Sanitarias (ISCIII-FIS PI 12/0615). P.M. is also supported by MINECO (SAF2013/43065), ERANET E-Rare (PI112/03112) and Fundación Sandra Ibarra. P.M. also acknowledges the supports from Obra Social "La Caixa/Fundacio "Josep Carreras". The IUOPA is supported by the Obra Social Cajastur, Spain.

Figure legends

Figure1. DNA methylation changes during MSC aging. (A) Unsupervised hierarchical clustering and heatmap including the 15000 most variable CpG sites with differential DNA methylation between *young* and *old* MSCs. Average methylation values are displayed from 0 (blue) to 1 (yellow). (B) Density plot for differentially methylated CpG sites between representative *young* (two years old; 2-yo) and *old* (87 years old; 87-yo) MSCs. (C) Distribution of differentially methylated CpGs relative to CpG Island. (D) Relative distribution of differentially methylated CpGs across different genomic regions. (E) Examples of aging-specific CpG methylation in particular genes further validated by pyrosequencing in an independent set of samples. For each of the genes of interest, a scatter plot of the percentage of methylation obtained for each sample and CpG of interest is shown. The two genes at the top show an age-dependent hypermethylation tendency, while the three genes at the bottom show hypomethylation with respect to age. Each point represents a single observation for a given sample and CpG of interest. The blue line represents a linear model fit. A 0.95 confidence interval of the fitted model is shown in gray. (F) Venn diagrams showing the number of CpG sites (hyper- and hypomethylated) shared by the different tissues

Figure2. Chromatin signatures associated with DNA methylation changes during aging. (A) Heatmaps showing significant enrichment of hyper- and hypomethylated CpG sites, identified in MSCs, blood, neurons and glia, with different histone marks and chromatin modifiers contained in the UCSC Genome Browser Broad Histone track from the ENCODE Project. Color code indicates the significant enrichment based on $\log_2$ odds ratio (OR). (B) Circular representation of three representative chromosomes (1, 6, and 17), indicating whether the CpGs were hypermethylated (red) or hypomethylated (blue) during MSC aging. Inner tracks display chromatin marks (H3K4me1, H3K9me3, H3K27me3, and EZH2), generated for HUVEC cells, and associated with differentially methylated regions during aging. Broad histone peak information was averaged in 200 kbp genomic windows and represented as histogram tracks. Three examples of hypo- and hypermethylated DNA regions associated with specific chromatin signatures are displayed below.

Figure3. Interindividual DNA methylation variability during MSC aging. (A) Density plot for CpG sites showing significant changes in variance in *young* and *old* MSCs. (B)

Bar plot showing the number of age-dependent heteroscedastic (convergent and divergent) and homoscedastic (high (HV) and low (LV) variability) CpG sites in MSCs. (C) Box plots showing the classification of CpG sites into different groups based on the aging-dependent behavior of the interindividual variability. Representative examples of CpG sites for each group are shown below (mvalue: relative methylation values). (D) Distribution of homoscedastic and heteroscedastic CpGs relative to CpG island status and relative distribution across different genomic regions.

Figure4. Interindividual DNA methylation variability during aging of blood cells. (A) Density plot for CpG sites showing significant changes of variance in *young* and *old* individuals. (B) Bar plot showing the number of age-dependent heteroscedastic (convergent and divergent) and homoscedastic (high (HV) and low (LV) variability) CpG sites. (C) Box plots showing the classification of the CpG sites in different groups based on the aging-dependent behavior of the interindividual variability.

Figure5. Role of genetic factors in interindividual DNA methylation variability during aging. (A) Density plot for CpG sites showing significant changes of methylation variance in blood cells of MZ twins during aging. (B) Density plot for comparison between the mean Euclidean distance ($\overline{\delta}$) and the interindividual variability (σ^2) in methylation values between *old* and *young* MZ twins. The horizontal dotted lines represent a 2 fold change in the $\overline{\delta}$ between MZ twins. (C) Circular representation of genome-wide CpG sites showing differences, in the $\overline{\delta}$ between methylation values of *young* and *old* MZ twins. δ was averaged using a 2Mbp window size. Inner tracks show genomic regions where the $\overline{\delta}$ was higher (blue region) or lower (green region) in *old* compared with *young* MZ twins. (D) Density plots for comparison between the $\overline{\delta}$ and the σ^2 in methylation values between *old* and *young* MZ twins, in hyper-, hypomethylated, heteroscedastic and homoscedastic CpGs.

References

Allegretta M, Nicklas JA, Sriram S, Albertini RJ. 1990. T cells responsive to myelin basic protein in patients with multiple sclerosis. *Science* **247**(4943): 718-721.

Bahar R, Hartmann CH, Rodriguez KA, Denny AD, Busuttil RA, Dolle ME, Calder RB, Chisholm GB, Pollock BH, Klein CA et al. 2006. Increased cell-to-cell variation in gene expression in ageing mouse heart. *Nature* **441**(7096): 1011-1014.

Beerman I, Bock C, Garrison BS, Smith ZD, Gu H, Meissner A, Rossi DJ. 2013. Proliferation-dependent alterations of the DNA methylation landscape underlie hematopoietic stem cell aging. *Cell Stem Cell* **12**(4): 413-425.

Bell JT, Tsai PC, Yang TP, Pidsley R, Nisbet J, Glass D, Mangino M, Zhai G, Zhang F, Valdes A et al. 2012. Epigenome-wide scans identify differentially methylated regions for age and age-related phenotypes in a healthy ageing population. *PLoS Genet* **8**(4): e1002629.

Bibikova M, Barnes B, Tsan C, Ho V, Klotzle B, Le JM, Delano D, Zhang L, Schroth GP, Gunderson KL et al. 2011. High density DNA methylation array with single CpG site resolution. *Genomics* **98**(4): 288-295.

Bird AP. 1986. CpG-rich islands and the function of DNA methylation. *Nature* **321**(6067): 209-213.

Bird AP, Wolffe AP. 1999. Methylation-induced repression--belts, braces, and chromatin. *Cell* **99**(5): 451-454.

Bjornsson HT, Cui H, Gius D, Fallin MD, Feinberg AP. 2004. The new field of epigenomics: implications for cancer and other common disease research. *Cold Spring Harb Symp Quant Biol* **69**: 447-456.

Bocker MT, Hellwig I, Breiling A, Eckstein V, Ho AD, Lyko F. 2011. Genome-wide promoter DNA methylation dynamics of human hematopoietic progenitor cells during differentiation and aging. *Blood* **117**(19): e182-189.

Bocklandt S, Lin W, Sehl ME, Sanchez FJ, Sinsheimer JS, Horvath S, Vilain E. 2011. Epigenetic predictor of age. *PLoS One* **6**(6): e14821.

Bork S, Pfister S, Witt H, Horn P, Korn B, Ho AD, Wagner W. 2010. DNA methylation pattern changes upon long-term culture and aging of human mesenchymal stromal cells. *Aging Cell* **9**(1): 54-63.

Calvanese V, Fernandez AF, Urdinguio RG, Suarez-Alvarez B, Mangas C, Perez-Garcia V, Bueno C, Montes R, Ramos-Mejia V, Martinez-Camblor P et al. 2012. A promoter DNA demethylation landscape of human hematopoietic differentiation. *Nucleic Acids Res* **40**(1): 116-131.

Calvanese V, Horrillo A, Hmadcha A, Suarez-Alvarez B, Fernandez AF, Lara E, Casado S, Menendez P, Bueno C, Garcia-Castro J et al. 2008. Cancer genes hypermethylated in human embryonic stem cells. *PLoS One* **3**(9): e3294.

Carlson M. TxDb.Hsapiens.UCSC.hg19.knownGene: Annotation package for TranscriptDb object(s). R package version 2.9.2.

Coolen MW, Statham AL, Qu W, Campbell MJ, Henders AK, Montgomery GW, Martin NG, Clark SJ. 2011. Impact of the genome on the epigenome is manifested in DNA methylation patterns of imprinted regions in monozygotic and dizygotic twins. *PLoS One* **6**(10): e25590.

Choi MR, In YH, Park J, Park T, Jung KH, Chai JC, Chung MK, Lee YS, Chai YG. 2012. Genome-scale DNA methylation pattern profiling of human bone marrow mesenchymal stem cells in long-term culture. *Exp Mol Med* **44**(8): 503-512.

Christensen BC, Houseman EA, Marsit CJ, Zheng S, Wrensch MR, Wiemels JL, Nelson HH, Karagas MR, Padbury JF, Bueno R et al. 2009. Aging and environmental exposures alter tissue-specific DNA methylation dependent upon CpG island context. *PLoS Genet* **5**(8): e1000602.

Day K, Waite LL, Thalacker-Mercer A, West A, Bamman MM, Brooks JD, Myers RM, Absher D. 2013. Differential DNA methylation with age displays both common and dynamic features across human tissues that are influenced by CpG landscape. *Genome Biol* **14**(9): R102.

Dedeurwaerder S, Defrance M, Calonne E, Denis H, Sotiriou C, Fuks F. 2011. Evaluation of the Infinium Methylation 450K technology. *Epigenomics* **3**(6): 771-784.

Dennis G, Jr., Sherman BT, Hosack DA, Yang J, Gao W, Lane HC, Lempicki RA. 2003. DAVID: Database for Annotation, Visualization, and Integrated Discovery. *Genome Biol* **4**(5): P3.

Du P, Zhang X, Huang C-C, Jafari N, Kibbe Wa, Hou L, Lin SM. 2010. Comparison of Beta-value and M-value methods for quantifying methylation levels by microarray analysis. *BMC Bioinformatics* **11**: 587.

Feil R, Fraga MF. 2012. Epigenetics and the environment: emerging patterns and implications. *Nat Rev Genet* **13**(2): 97-109.

Fernandez AF, Assenov Y, Martin-Subero JI, Balint B, Siebert R, Taniguchi H, Yamamoto H, Hidalgo M, Tan AC, Galm O et al. 2012. A DNA methylation fingerprint of 1628 human samples. *Genome Res* **22**(2): 407-419.

Fraga MF. 2009. Genetic and epigenetic regulation of aging. *Curr Opin Immunol* **21**(4): 446-453.

Fraga MF, Ballestar E, Paz MF, Ropero S, Setien F, Ballestar ML, Heine-Suner D, Cigudosa JC, Urioste M, Benitez J et al. 2005. Epigenetic differences arise during the lifetime of monozygotic twins. *Proc Natl Acad Sci U S A* **102**(30): 10604-10609.

Gage PJ, Kuang C, Zacharias AL. 2014. The homeodomain transcription factor PITX2 is required for specifying correct cell fates and establishing angiogenic privilege in the developing cornea. *Dev Dyn*.

Gemma C, Ramagopalan SV, Down TA, Beyan H, Hawa MI, Holland ML, Hurd PJ, Giovannoni G, David Leslie R, Ebers GC et al. 2013. Inactive or moderately active human promoters are enriched for inter-individual epialleles. *Genome Biol* **14**(5): R43.

Gertz J, Varley KE, Reddy TE, Bowling KM, Pauli F, Parker SL, Kucera KS, Willard HF, Myers RM. 2011. Analysis of DNA methylation in a three-generation family reveals widespread genetic influence on epigenetic regulation. *PLoS Genet* **7**(8): e1002228.

Gross S, Krause Y, Wuelling M, Vortkamp A. 2012. Hoxa11 and Hoxd11 regulate chondrocyte differentiation upstream of Runx2 and Shox2 in mice. *PLoS One* **7**(8): e43553.

Guintivano J, Aryee MJ, Kaminsky ZA. 2013. A cell epigenotype specific model for the correction of brain cellular heterogeneity bias and its application to age, brain region and major depression. *Epigenetics* **8**(3): 290-302.

Hannum G, Guinney J, Zhao L, Zhang L, Hughes G, Sadda S, Klotzle B, Bibikova M, Fan JB, Gao Y et al. 2013. Genome-wide methylation profiles reveal quantitative views of human aging rates. *Mol Cell* **49**(2): 359-367.

Hansen KD, Aryee M. minfi: Analyze Illumina's 450k methylation arrays. R package version 1.7.15.

Heijmans BT, Kremer D, Tobi EW, Boomsma DI, Slagboom PE. 2007. Heritable rather than age-related environmental and stochastic factors dominate variation in DNA methylation of the human IGF2/H19 locus. *Hum Mol Genet* **16**(5): 547-554.

Hernandez DG, Nalls MA, Gibbs JR, Arepalli S, van der Brug M, Chong S, Moore M, Longo DL, Cookson MR, Traynor BJ et al. 2011. Distinct DNA methylation changes highly correlated with chronological age in the human brain. *Hum Mol Genet* **20**(6): 1164-1172.

Heyn H, Li N, Ferreira HJ, Moran S, Pisano DG, Gomez A, Diez J, Sanchez-Mut JV, Setien F, Carmona FJ et al. 2012. Distinct DNA methylomes of newborns and centenarians. *Proc Natl Acad Sci U S A* **109**(26): 10522-10527.

Heyn H, Moran S, Esteller M. 2013. Aberrant DNA methylation profiles in the premature aging disorders Hutchinson-Gilford Progeria and Werner syndrome. *Epigenetics* **8**(1): 28-33.

Horvath S, Zhang Y, Langfelder P, Kahn RS, Boks MP, van Eijk K, van den Berg LH, Ophoff RA. 2012. Aging effects on DNA methylation modules in human brain and blood tissue. *Genome Biol* **13**(10): R97.

Houseman EA, Accomando WP, Koestler DC, Christensen BC, Marsit CJ, Nelson HH, Wiencke JK, Kelsey KT. 2012. DNA methylation arrays as surrogate measures of cell mixture distribution. *BMC Bioinformatics* **13**: 86.

Huang da W, Sherman BT, Lempicki RA. 2009. Systematic and integrative analysis of large gene lists using DAVID bioinformatics resources. *Nat Protoc* **4**(1): 44-57.

Issa JP. 2014. Aging and epigenetic drift: a vicious cycle. *J Clin Invest* **124**(1): 24-29.

Jaenisch R, Bird A. 2003. Epigenetic regulation of gene expression: how the genome integrates intrinsic and environmental signals. *Nat Genet* **33 Suppl**: 245-254.

Jeong S, Liang G, Sharma S, Lin JC, Choi SH, Han H, Yoo CB, Egger G, Yang AS, Jones PA. 2009. Selective anchoring of DNA methyltransferases 3A and 3B to nucleosomes containing methylated DNA. *Mol Cell Biol* **29**(19): 5366-5376.

Johansson A, Enroth S, Gyllensten U. 2013. Continuous Aging of the Human DNA Methylome Throughout the Human Lifespan. *PLoS One* **8**(6): e67378.

Jones A, Teschendorff AE, Li Q, Hayward JD, Kannan A, Mould T, West J, Zikan M, Cibula D, Fiegl H et al. 2013. Role of DNA methylation and epigenetic silencing of HAND2 in endometrial cancer development. *PLoS Med* **10**(11): e1001551.

Kaminsky ZA, Tang T, Wang SC, Ptak C, Oh GH, Wong AH, Feldcamp LA, Virtanen C, Halfvarson J, Tysk C et al. 2009. DNA methylation profiles in monozygotic and dizygotic twins. *Nat Genet* **41**(2): 240-245.

Köster J, Rahmann S. 2012. Snakemake--a scalable bioinformatics workflow engine. *Bioinformatics (Oxford, England)* **28**: 2520-2522.

Krzywinski M, Schein J, Birol I, Connors J, Gascoyne R, Horsman D, Jones SJ, Marra MA. 2009. Circos: an information aesthetic for comparative genomics. *Genome Res* **19**(9): 1639-1645.

Leek JT, Johnson WE, Parker HS, Jaffe AE, Storey JD. sva: Surrogate Variable Analysis. R package version 3.7.0.

Lemire M, Butcher DT, Grafodatskaya D, Zanke BW, Weksberg R. 2013. Discovery of cross-reactive probes and polymorphic CpGs in the Illumina Infinium HumanMethylation450 microarray. 203-209.

Lister R, Mukamel EA, Nery JR, Urich M, Puddifoot CA, Johnson ND, Lucero J, Huang Y, Dwork AJ, Schultz MD et al. 2013. Global epigenomic reconfiguration during mammalian brain development. *Science* **341**(6146): 1237905.

Liu Y, Aryee MJ, Padyukov L, Fallin MD, Hesselberg E, Runarsson A, Reinius L, Acevedo N, Taub M, Ronninger M et al. 2013. Epigenome-wide association data implicate DNA methylation as an intermediary of genetic risk in rheumatoid arthritis. *Nat Biotechnol* **31**(2): 142-147.

Makismovic J, Gordon L, Oshlack A. 2012. SWAN: Subset-quantile within array normalization for Illumina Infinium HumanMethylation450 BeadChips. *Genome Biology*.

Martino D, Loke YJ, Gordon L, Ollikainen M, Cruickshank MN, Saffery R, Craig JM. Longitudinal, genome-scale analysis of DNA methylation in twins from birth to 18 months of age reveals rapid epigenetic change in early life and pair-specific effects of discordance. *Genome Biol* **14**(5): R42.

Numata S, Ye T, Hyde TM, Guitart-Navarro X, Tao R, Wininger M, Colantuoni C, Weinberger DR, Kleinman JE, Lipska BK. 2012. DNA methylation signatures in development and aging of the human prefrontal cortex. *Am J Hum Genet* **90**(2): 260-272.

Ollikainen M, Smith KR, Joo EJ, Ng HK, Andronikos R, Novakovic B, Abdul Aziz NK, Carlin JB, Morley R, Saffery R et al. 2010. DNA methylation analysis of multiple tissues from newborn twins reveals both genetic and intrauterine components to variation in the human neonatal epigenome. *Hum Mol Genet* **19**(21): 4176-4188.

Ong ML, Holbrook JD. 2013. Novel region discovery method for Infinium 450K DNA methylation data reveals changes associated with ageing in muscle and neuronal pathways. *Aging Cell*.

Pan KH, Lih CJ, Cohen SN. 2005. Effects of threshold choice on biological conclusions reached during analysis of gene expression by DNA microarrays. *Proc Natl Acad Sci U S A* **102**(25): 8961-8965.

Pirazzini C, Giuliani C, Bacalini MG, Boattini A, Capri M, Fontanesi E, Marasco E, Mantovani V, Pierini M, Pini E et al. 2012. Space/population and time/age in DNA methylation variability in humans: a study on IGF2/H19 locus in different Italian populations and in mono- and di-zygotic twins of different age. *Aging (Albany NY)* **4**(7): 509-520.

Pollina EA, Brunet A. 2011. Epigenetic regulation of aging stem cells. *Oncogene* **30**(28): 3105-3126.

Rada-Iglesias A, Bajpai R, Swigut T, Brugmann SA, Flynn RA, Wysocka J. 2010. A unique chromatin signature uncovers early developmental enhancers in humans. *Nature* **470**(7333): 279-283.

Rakyan VK, Down TA, Maslau S, Andrew T, Yang TP, Beyan H, Whittaker P, McCann OT, Finer S, Valdes AM et al. 2010. Human aging-associated DNA hypermethylation occurs preferentially at bivalent chromatin domains. *Genome Res* **20**(4): 434-439.

Rauch T, Li H, Wu X, Pfeifer GP. 2006. MIRA-assisted microarray analysis, a new technology for the determination of DNA methylation patterns, identifies frequent methylation of homeodomain-containing genes in lung cancer cells. *Cancer Res* **66**(16): 7939-7947.

Rosenbloom KR, Dreszer TR, Long JC, Malladi VS, Sloan CA, Raney BJ, Cline MS, Karolchik D, Barber GP, Clawson H et al. 2012. ENCODE whole-genome data in the UCSC Genome Browser: update 2012. *Nucleic Acids Res* **40**(Database issue): D912-917.

Rosenbloom KR, Dreszer TR, Pheasant M, Barber GP, Meyer LR, Pohl A, Raney BJ, Wang T, Hinrichs AS, Zweig AS et al. 2010. ENCODE whole-genome data in the UCSC Genome Browser. *Nucleic Acids Res* **38**(Database issue): D620-625.

Sharpless NE, DePinho RA. 2004. Telomeres, stem cells, senescence, and cancer. *J Clin Invest* **113**(2): 160-168.

Sherry ST, Ward MH, Kholodov M, Baker J, Phan L, Smigielski EM, Sirotkin K. 2001. dbSNP: the NCBI database of genetic variation. *Nucleic acids research* **29**: 308-311.

Singh MK, Petry M, Haenig B, Lescher B, Leitges M, Kispert A. 2005. The T-box transcription factor Tbx15 is required for skeletal development. *Mech Dev* **122**(2): 131-144.

Smyth GK. 2005. limma: Linear Models for Microarray Data. In *Bioinformatics and Computational Biology Solutions Using R and Bioconductor*, pp. 397-420.

Stolzing A, Jones E, McGonagle D, Scutt A. 2008. Age-related changes in human bone marrow-derived mesenchymal stem cells: consequences for cell therapies. *Mech Ageing Dev* **129**(3): 163-173.

Taiwo O, Wilson GA, Emmett W, Morris T, Bonnet D, Schuster E, Adejumo T, Beck S, Pearce DJ. 2013. DNA methylation analysis of murine hematopoietic side population cells during aging. *Epigenetics* **8**(10).

Talens RP, Christensen K, Putter H, Willemsen G, Christiansen L, Kremer D, Suchiman HE, Slagboom PE, Boomsma DI, Heijmans BT. 2012. Epigenetic variation during the adult lifespan: cross-sectional and longitudinal data on monozygotic twin pairs. *Aging Cell* **11**(4): 694-703.

Teschendorff AE, Menon U, Gentry-Maharaj A, Ramus SJ, Weisenberger DJ, Shen H, Campan M, Noushmehr H, Bell CG, Maxwell AP et al. 2010. Age-dependent DNA methylation of genes that are suppressed in stem cells is a hallmark of cancer. *Genome Res* **20**(4): 440-446.

Timp W, Feinberg AP. 2013. Cancer as a dysregulated epigenome allowing cellular growth advantage at the expense of the host. *Nat Rev Cancer* **13**(7): 497-510.

Tong WG, Wierda WG, Lin E, Kuang SQ, Bekele BN, Estrov Z, Wei Y, Yang H, Keating MJ, Garcia-Manero G. 2010. Genome-wide DNA methylation profiling of chronic lymphocytic leukemia allows identification of epigenetically repressed molecular pathways with clinical impact. *Epigenetics* **5**(6): 499-508.

Triche TJ. 2013. FDb.InfiniumMethylation.hg19: Annotation package for Illumina Infinium DNA methylation array probes. R package version 1.0.1.

van Dongen J, Slagboom PE, Draisma HH, Martin NG, Boomsma DI. 2012. The continuing value of twin studies in the omics era. *Nat Rev Genet* **13**(9): 640-653.

Wong CC, Caspi A, Williams B, Craig IW, Houts R, Ambler A, Moffitt TE, Mill J. 2010. A longitudinal study of epigenetic variation in twins. *Epigenetics* **5**(6): 516-526.

Wu H, Caffo B, Jaffee HA, Irizarry RA, Feinberg AP. 2010. Redefining CpG islands using hidden Markov models. *Biostatistics* **11**(3): 499-514.

Xie M, Hong C, Zhang B, Lowdon RF, Xing X, Li D, Zhou X, Lee HJ, Maire CL, Ligon KL et al. 2013. DNA hypomethylation within specific transposable

element families associates with tissue-specific enhancer landscape. *Nat Genet* **45**(7): 836-841.

Zykovich A, Hubbard A, Flynn JM, Tarnopolsky M, Fraga MF, Kerksick C, Ogborn D, MacNeil L, Mooney SD, Melov S. 2014. Genome-wide DNA methylation changes with age in disease-free human skeletal muscle. *Aging Cell* **13**(2): 360-366.

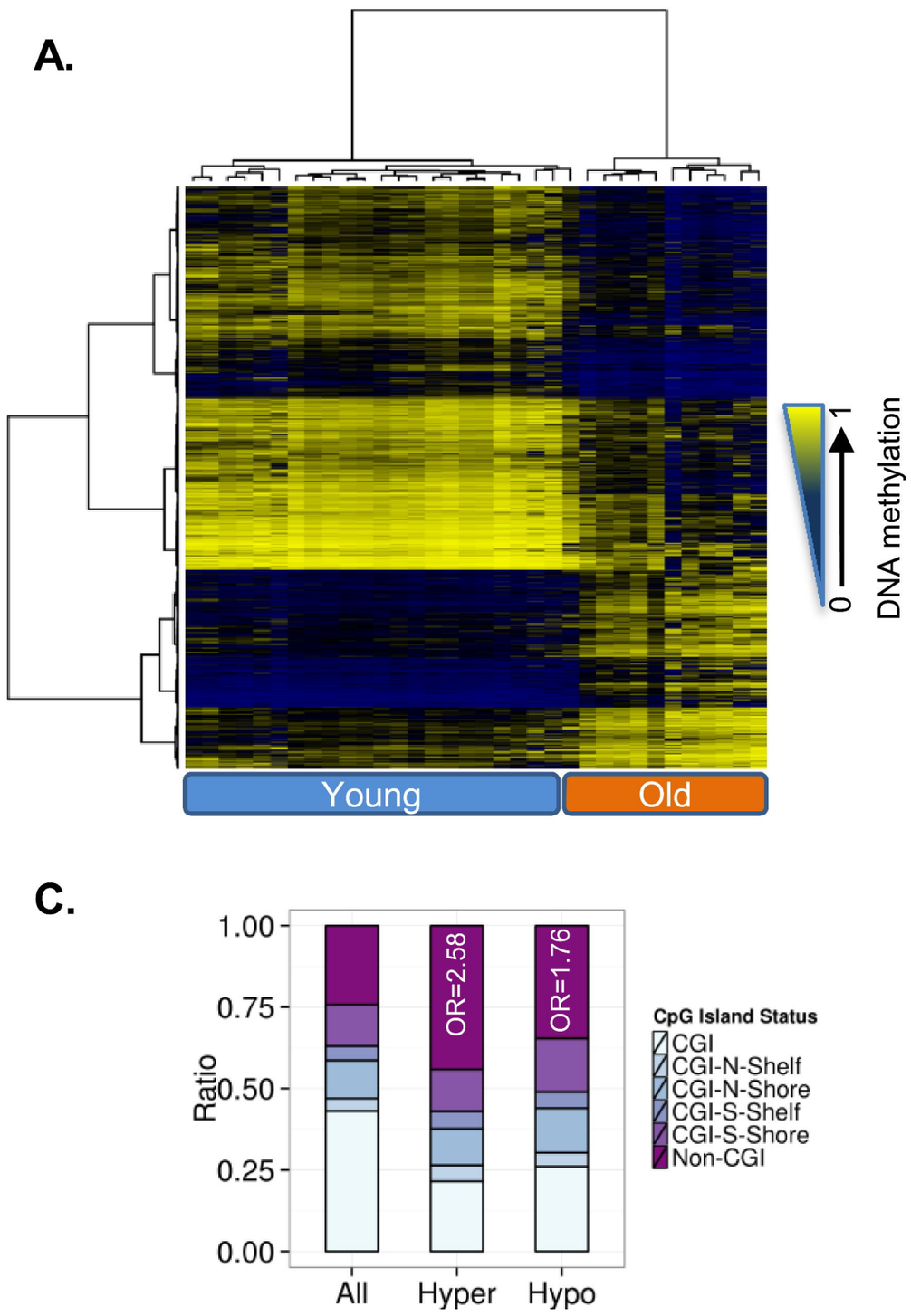

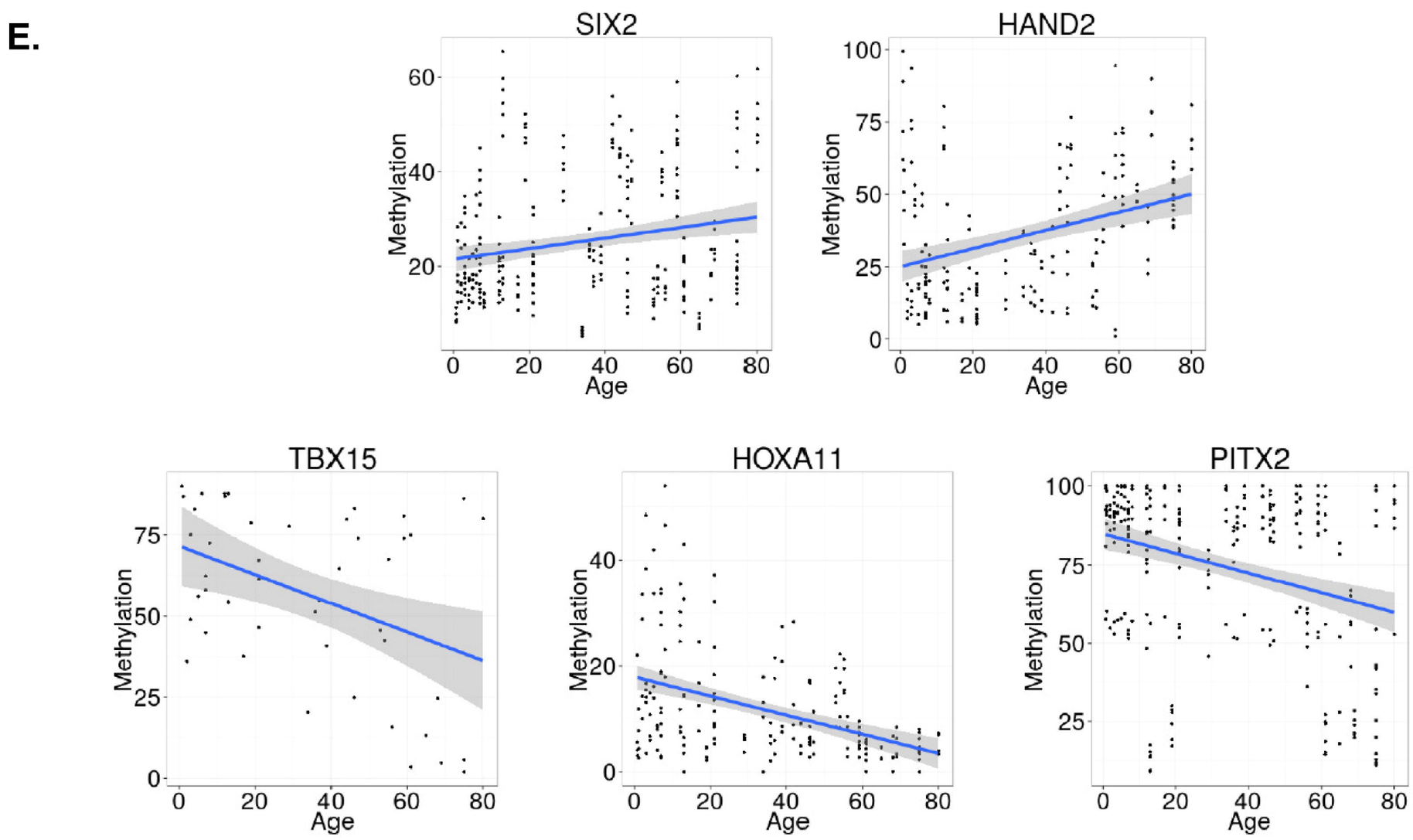

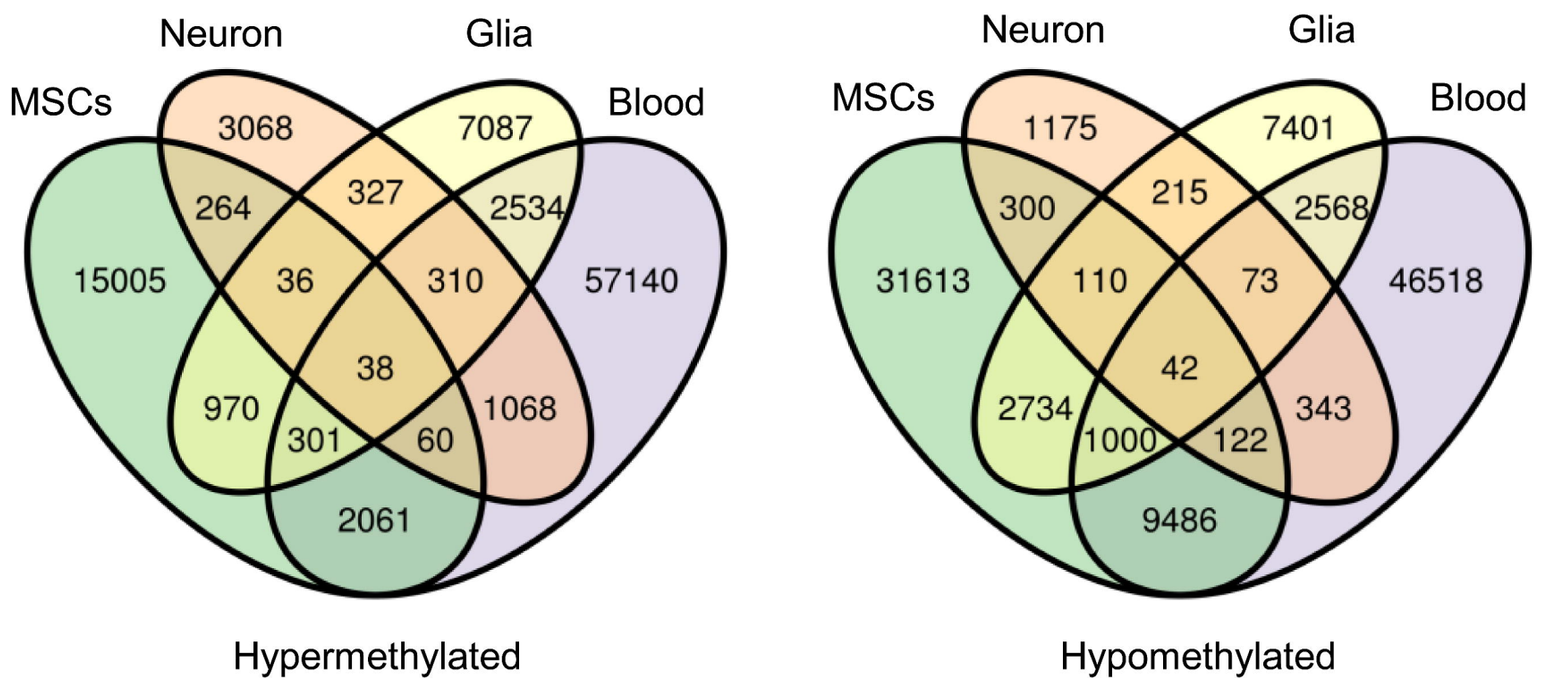

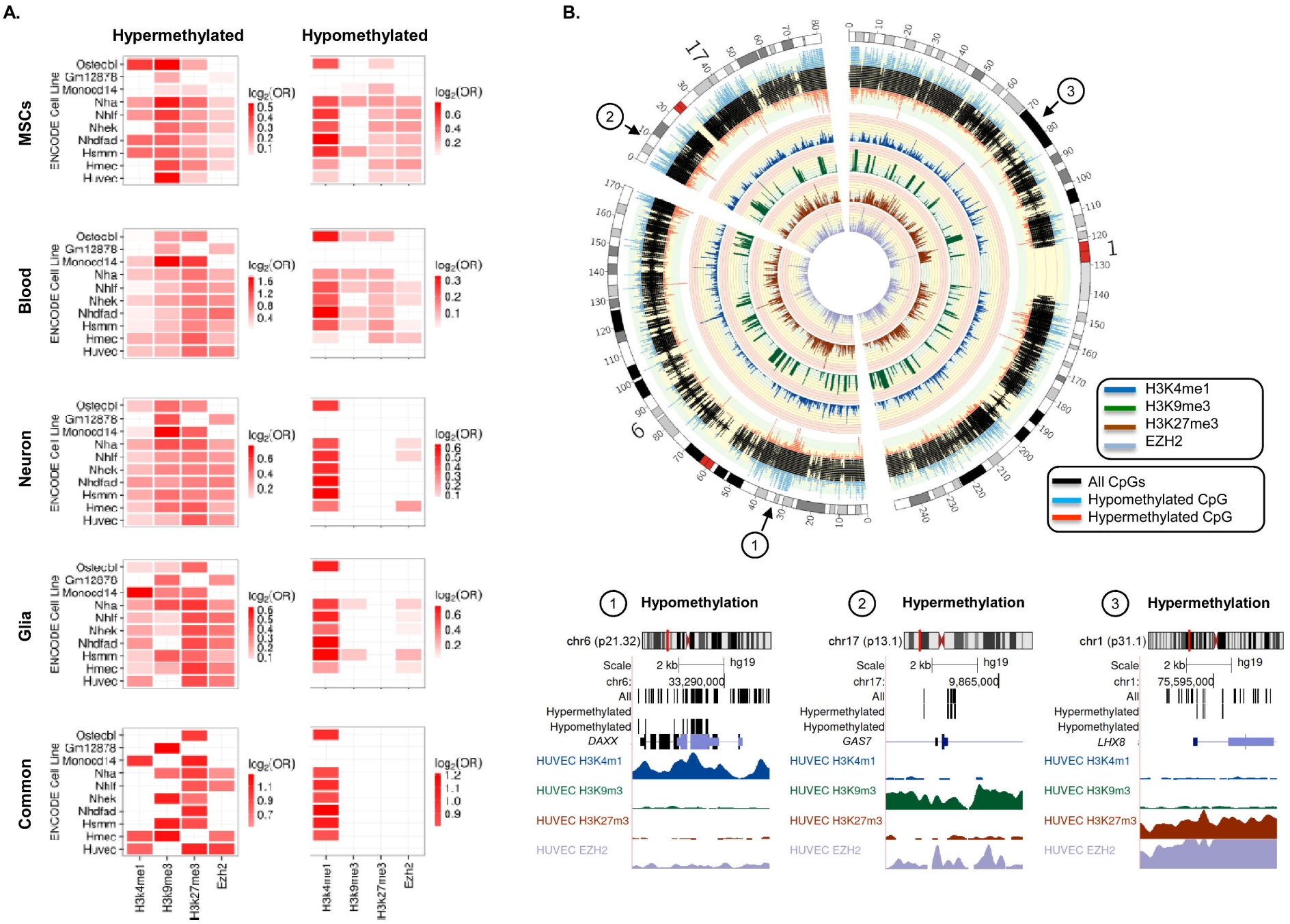
A.
Hypermethylated
Hypomethylated
MSCs
Blood
Neuron
Glia
Common
ENCODE Cell Line
Osteobl
Gm12878
Monocd14
Nha
Nhlf
Nhek
Nhdfad
Hsmm
Hmec
Huvec
log2(OR)
H3k4me1
H3k9me3
H3k27me3
Ezh2
B.
H3K4me1
H3K9me3
H3K27me3
EZH2
All CpGs
Hypomethylated CpG
Hypermethylated CpG
1 Hypomethylation
2 Hypermethylation
3 Hypermethylation
chr6 (p21.32)
chr17 (p13.1)
chr1 (p31.1)
Scale
2 kb
hg19
chr6:
33,290,000
chr17:
9,865,000
chr1:
75,595,000
All
Hypermethylated
Hypomethylated
DAXX
GAS7
LHX8
HUVEC H3K4m1
HUVEC H3K9m3
HUVEC H3K27m3
HUVEC EZH2

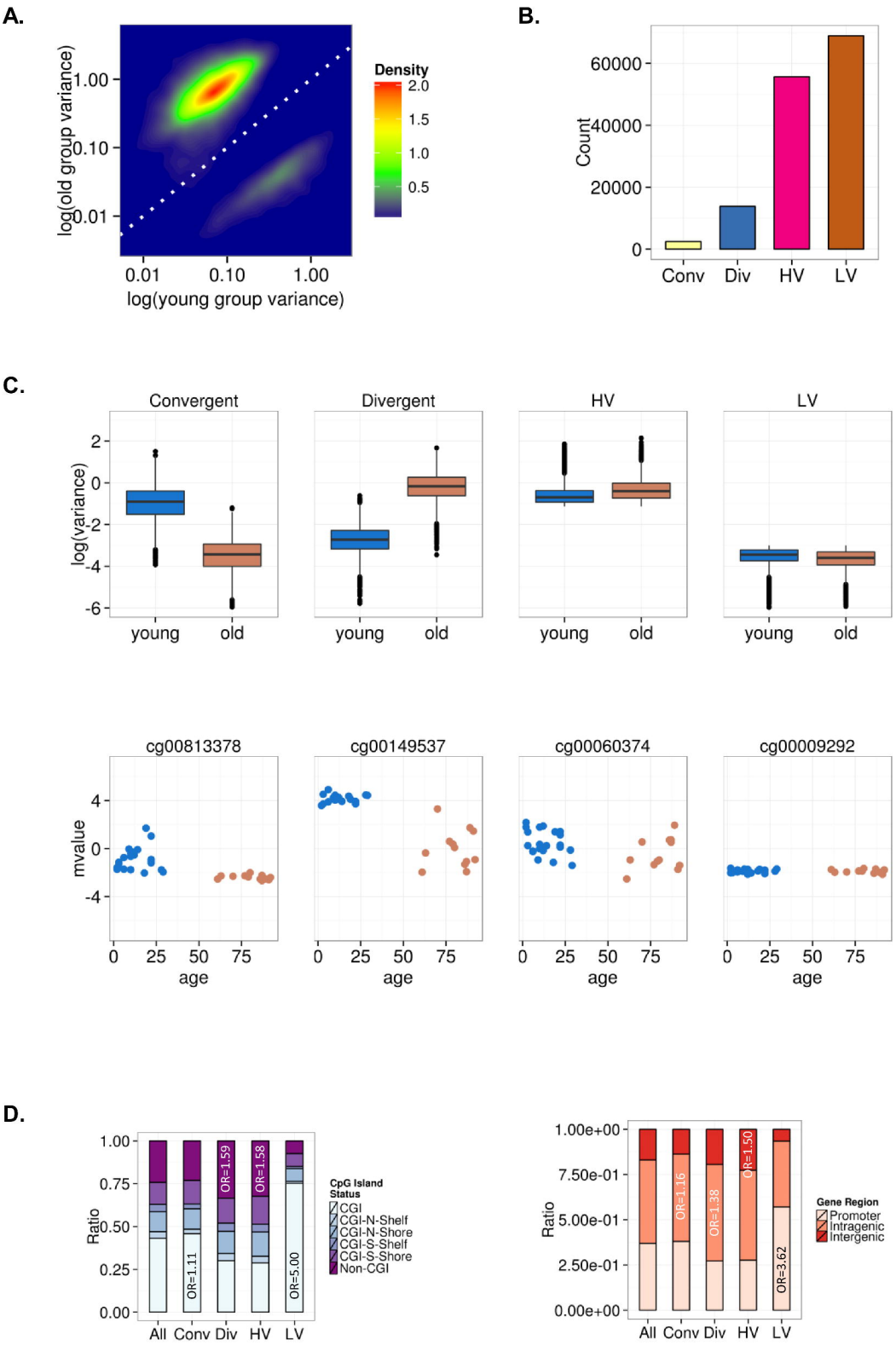
A.
log(old group variance)
log(young group variance)
Density
B.
Count
Conv
Div
HV
LV
C.
Convergent
Divergent
HV
LV
log(variance)
young
old
cg00813378
cg00149537
cg00060374
cg00009292
mvalue
age
D.
Ratio
CpG Island Status
CGI
CGI-N-Shelf
CGI-N-Shore
CGI-S-Shelf
CGI-S-Shore
Non-CGI
OR=1.11
OR=1.59
OR=1.58
OR=5.00
All
Conv
Div
HV
LV
Gene Region
Promoter
Intragenic
Intergenic
OR=1.16
OR=1.38
OR=1.50
OR=3.62

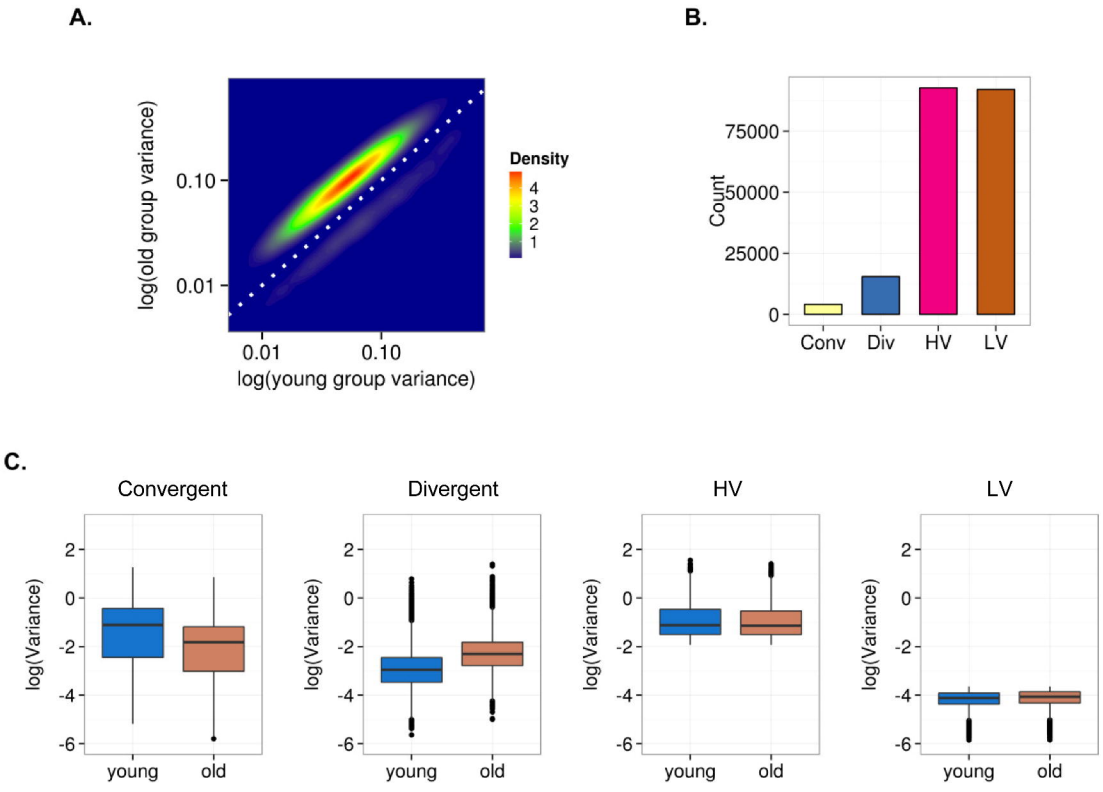
A.
log(old group variance)
0.10
0.01
0.01
0.10
log(young group variance)
Density
4
3
2
1
B.
Count
75000
50000
25000
0
Conv
Div
HV
LV
C.
Convergent
Divergent
HV
LV
log(Variance)
2
0
-2
-4
-6
young
old

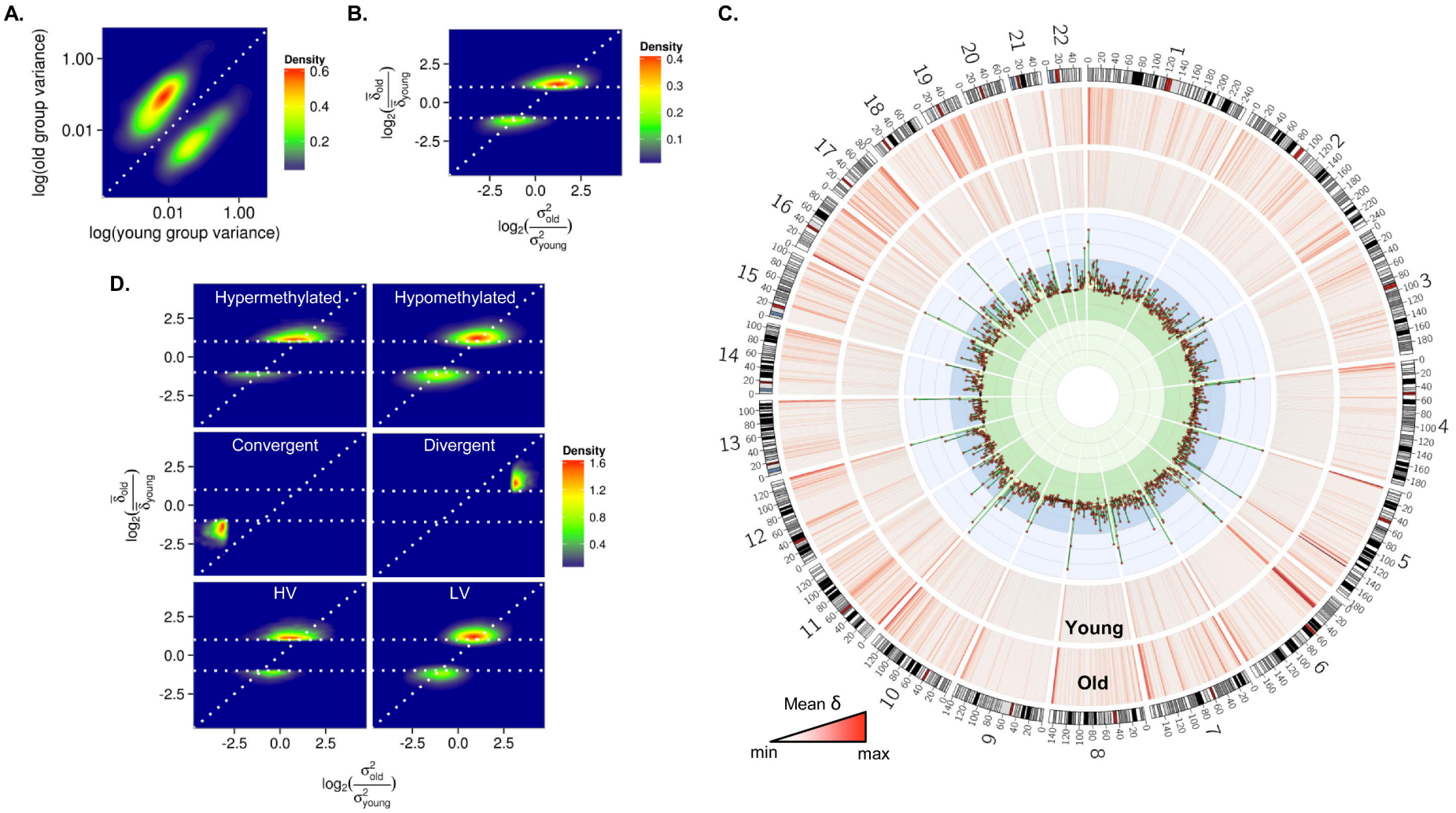
A.
log(old group variance)
log(young group variance)
1.00
0.01
0.01
1.00
Density
0.6
0.4
0.2
B.
Density
0.4
0.3
0.2
0.1
2.5
0.0
-2.5
-2.5
0.0
2.5
C.
Young
Old
Mean δ
min
max
D.
Hypermethylated
Hypomethylated
Convergent
Divergent
HV
LV
Density
1.6
1.2
0.8
0.4